

# Incompatible Magnetic Order in Multiferroic Hexagonal DyMnO<sub>3</sub>

C. Wehrenfennig,<sup>1</sup> D. Meier,<sup>1</sup> Th. Lottermoser,<sup>1</sup> Th. Lonkai,<sup>2</sup> J.-U.

Hoffmann,<sup>3</sup> N. Aliouane,<sup>3</sup> D. N. Argyriou,<sup>3</sup> and M. Fiebig<sup>1,\*</sup>

<sup>1</sup>*HISKP, Universität Bonn, Nussallee 14-16, 53115 Bonn, Germany*

<sup>2</sup>*Ganerben-Gymnasium, Mühlbergstraße 65, 74653 Künzelsau, Germany and*

<sup>3</sup>*Helmholtz-Zentrum Berlin für Materialien und Energie,*

*Glienicker Straße 100, 14109 Berlin, Germany*

(Dated: Dated March 22, 2021)

## Abstract

Magnetic order of the manganese and rare-earth lattices according to different symmetry representations is observed in multiferroic hexagonal (h-) DyMnO<sub>3</sub> by optical second harmonic generation and neutron diffraction. The incompatibility reveals that the  $3d-4f$  coupling in the h-RMnO<sub>3</sub> system ( $R = \text{Sc, Y, In, Dy} - \text{Lu}$ ) is substantially less developed than commonly expected. As a consequence, magnetoelectric coupling effects in this type of split-order parameter multiferroic that were previously assigned to a pronounced  $3d-4f$  coupling have now to be scrutinized with respect to their origin.

PACS numbers: 75.85.+t, 75.30.Et, 75.25.-j, 42.65.Ky

Controlling magnetism by electric fields and (di)electric properties by magnetic fields poses a great challenge to contemporary condensed-matter physics. Possibly the most fertile source for such “magnetoelectric” cross correlations are compounds with a coexistence of magnetic and electric long-range order, called multiferroics [2]. In the *joint-order-parameter multiferroics* the magnetic and the ferroelectric order are related to the same order parameter [3]. Although this leads to very pronounced magnetoelectric interactions the improper spontaneous polarization is extremely small ( $\ll 1 \mu\text{C}/\text{cm}^2$ ). In the *split-order-parameter multiferroics* magnetic and ferroelectric order emerge independently. Therefore, they display a technologically feasible proper spontaneous polarization of  $1 - 100 \mu\text{C}/\text{cm}^2$ . Aside from the ambient multiferroic  $\text{BiFeO}_3$  [4] a split-order-parameter system at the center of intense discussion is hexagonal (h-)  $\text{RMnO}_3$  with  $R = \text{Sc}, \text{Y}, \text{In}, \text{Dy-Lu}$  [5]. The system displays a variety of multiferroic phases and a “giant” magnetoelectric effect [6]. The availability of as many as nine h- $\text{RMnO}_3$  compounds is ideal for investigating the role played by magnetic  $3d-4f$  interactions in the manifestation of magnetoelectric effects, a key question of multiferroics research.

Thus far, it is assumed that the  $3d-4f$  interaction in the h- $\text{RMnO}_3$  system is strong with a rigid correlation between the magnetic  $\text{Mn}^{3+}$  and  $R^{3+}$  order [7–11]. The  $\text{Mn}^{3+}-R^{3+}$  exchange paths are affected by the ferroelectric distortion of the unit cell so that it is expected that, reminiscent of the orthorhombic manganites [3], the  $3d-4f$  interaction has substantial impact on the magnetoelectric behavior, including giant magnetoelectric [6] and magnetoelastic [12, 13] effects.

In this Letter we show that the  $3d-4f$  coupling in h- $\text{RMnO}_3$  is substantially less developed than assumed up to now. This is concluded from optical second harmonic generation (SHG) and neutron-diffraction data revealing that the  $\text{Mn}^{3+}$  spins and the  $\text{Dy}^{3+}$  spins in h- $\text{DyMnO}_3$  order according to different symmetry representations unless magnetization fields are present. This has extensive consequences for the magnetic structure and the magnetoelectric interactions in the multiferroic h- $\text{RMnO}_3$  system that are discussed in detail.

The h- $\text{RMnO}_3$  compounds display ferroelectric ordering at  $T_C = 650 - 990 \text{ K}$ , antiferromagnetic  $\text{Mn}^{3+}$  ordering at  $T_N = 66 - 130 \text{ K}$  [5], and, for  $R = \text{Dy-Yb}$ , magnetic  $R^{3+}$  ordering and reordering at  $T_N$  and  $4 - 8 \text{ K}$ , respectively [5, 7, 9, 10, 14]. The spontaneous polarization is  $5.6 \mu\text{C}/\text{cm}^2$  and directed along  $z$ . Frustration leads to a variety of triangular antiferromagnetic structures of the  $\text{Mn}^{3+}$  spins in the basal  $xy$  plane. In contrast, the  $R^{3+}$  sublattices order Ising-like along the hexagonal  $z$  axis. The possible magnetic structures of the  $\text{Mn}^{3+}$  and  $\text{Dy}^{3+}$  lattices correspond to four one-dimensional representations [15] that are compared in Table I. An exten-

sive investigation of the magnetic  $R^{3+}$  order commenced only recently [7, 9, 14, 16] and revealed that in h-HoMnO<sub>3</sub> and h-YbMnO<sub>3</sub> the Mn<sup>3+</sup> and the  $R^{3+}$  ordering occurs according to the same magnetic representation.

The compound with the smallest  $R^{3+}$  ion in the h-RMnO<sub>3</sub> series is h-DyMnO<sub>3</sub> which was grown for the first time only recently [17]. The magnetic structure of the Dy<sup>3+</sup> lattice was investigated by resonant x-ray diffraction and magnetization measurements [14, 17]. Its magnetic point group was found to be  $P\bar{6}_3cm$  in the interval  $10 \text{ K} < T < T_N$  (“high-temperature range”). At  $T < 10 \text{ K}$  (“low-temperature range”) or above a critical magnetic field applied along  $z$  it changes to  $P6_3cm$ . In this work we focus on the determination of the complementary Mn<sup>3+</sup> order, but for confirmation the Dy<sup>3+</sup> order is also verified.

SHG is described by the equation  $P_i(2\omega) = \epsilon_0 \chi_{ijk} E_j(\omega) E_k(\omega)$ . An electromagnetic light field  $\vec{E}$  at frequency  $\omega$  is incident on a crystal, inducing a dipole oscillation  $\vec{P}(2\omega)$ , which acts as source of a frequency-doubled light wave of the intensity  $I_{\text{SHG}} \propto |\vec{P}(2\omega)|^2$ . The susceptibility  $\chi_{ijk}$  couples incident light fields with polarizations  $j$  and  $k$  to a SHG contribution with polarization  $i$ . The magnetic and crystallographic symmetry of a compound uniquely determines the set of nonzero components  $\chi_{ijk}$  [18, 19]. In turn, observation of  $\chi_{ijk} \neq 0$  allows one to derive the the magnetic symmetry and structure.

The h-DyMnO<sub>3</sub> samples were obtained by the floating zone technique and verified for the absence of twinning and secondary phases by Laue diffraction. SHG reflection spectroscopy with 120-fs laser pulses was conducted on polished  $z$ -oriented crystals in a <sup>4</sup>He-operated cryostat generating magnetic fields of up to 8 T [19]. Neutron diffraction in the  $(h0l)$  plane was conducted at the E2 beamline of the Helmholtz-Zentrum at a wavelength of 2.39 Å with the sample mounted in a <sup>3</sup>He/<sup>4</sup>He dilution insert.

In Table I the calculated selection rules identifying the magnetic structure of the Mn<sup>3+</sup> and Dy<sup>3+</sup> lattice are listed. SHG is only sensitive to the Mn<sup>3+</sup> order with  $\chi_{xxx}$  and  $\chi_{yyy}$  as independent tensor components [18]. Neutron diffraction can probe the magnetic moments of Mn<sup>3+</sup> and Dy<sup>3+</sup>. The (100) and (101) reflections lead to very clear selection rules so that we restrict the discussion to them. The contributions by the Mn<sup>3+</sup> and Dy<sup>3+</sup> lattice to these reflections were separated by setting the magnetic moment of the other lattice, respectively, to zero in the computations done with *Simref* 2.6 [9].

We first focus on the high-temperature range and measurements at zero magnetic field. Figure 1 shows the analysis of the magnetic structure of the Mn<sup>3+</sup> lattice by SHG spectroscopy. Because of

the large optical absorption the SHG data on h-DyMnO<sub>3</sub> cannot be taken with the standard transmission setup and ns laser pulses [19] — in contrast to all other h-RMnO<sub>3</sub> compounds. Instead the reflected SHG signal was measured with a fs laser system. With fs laser pulses, higher-order SHG contributions, incoherent multiphoton processes, and ultrafast nonequilibrium effects can easily obscure any magnetically induced SHG [19, 20]. In the first step we therefore had to verify to what extent SHG is still a feasible probe for the magnetic structure. We chose h-HoMnO<sub>3</sub> for this test since it allows us to compare transmission and reflection data. Figure 1(a) shows the SHG transmission spectrum taken at two different temperatures with a fs laser system. Aside from a minor decrease of resolution the fs laser pulses lead to the same SHG spectra as the ns laser pulses [19]. With SHG from  $\chi_{xxx}$  at 50 K and from  $\chi_{yyy}$  at 10 K we identify the  $P\bar{6}_3cm$  and the  $P\bar{6}_3c\bar{m}$  structure, respectively, on the basis of Table I. Note that the spectral dependence is also characteristic for the respective phases [21]. Figure 1(b) shows the corresponding SHG reflection spectra. Aside from a 98% decrease of the SHG yield the result remains unchanged. Hence, the fs reflection data are well suited for identifying the magnetic phase of h-RMnO<sub>3</sub> by SHG.

Figures 1(c) and 1(d) show the spectral and temperature dependence of the SHG signal in h-DyMnO<sub>3</sub> in a fs reflection experiment. Comparison with Fig. 1(b) and Table I clearly reveals  $P\bar{6}_3cm$  as magnetic symmetry of the Mn<sup>3+</sup> lattice in the high-temperature range up to  $T_N = 66$  K. This is an utterly surprising result because  $P\bar{6}_3c\bar{m}$  does not match the  $P\bar{6}_3c\bar{m}$  symmetry of the Dy<sup>3+</sup> lattice proposed in Ref. 14. We therefore sought additional confirmation by neutron diffraction.

In Fig. 2 we show the temperature dependence of the (101) and (100) reflections of h-DyMnO<sub>3</sub>. Note that while the (101) reflection is magnetically induced the (100) reflection in the high-temperature range is entirely due to crystallographic contributions — its magnetic intensity is zero. According to Table I, this is only possible if the magnetic symmetry of the Mn<sup>3+</sup> lattice is either  $P\bar{6}_3cm$  or  $P6_3c\bar{m}$  of which the latter corresponds to a ferromagnetic state which is ruled out by magnetization measurements [8, 14, 17]. Table I further shows that the magnetic symmetry of the Dy<sup>3+</sup> lattice can only be  $P\bar{6}_3c\bar{m}$  which confirms the magnetic structure proposed earlier [14].

We thus conclude that three independent experimental parameters, i.e., SHG polarization, SHG spectrum, and neutron diffraction intensity, confirm  $P\bar{6}_3cm$  as magnetic symmetry of the Mn<sup>3+</sup> lattice in the high-temperature range of h-DyMnO<sub>3</sub>. This is in striking contrast to the known [14]  $P\bar{6}_3c\bar{m}$  symmetry of the Dy<sup>3+</sup> lattice which is confirmed by our neutron data. Hence, the Mn<sup>3+</sup> and the Dy<sup>3+</sup> order are “incompatible” in the sense of belonging to different magnetic representations.

Although it is not unusual that magnetic order is parametrized by more than one representation

it is most remarkable that this occurs in the h-RMnO<sub>3</sub> system. Up to now, research on this system was based on the assumption that a pronounced coupling between the Mn<sup>3+</sup> and R<sup>3+</sup> lattices is a central mechanism in determining its magnetoelectric and multiferroic properties [6–12]. Accordingly, ordering of the 3*d* and 4*f* lattices according to a single representation was implied to be compulsory. However, the incompatibility observed here shows that the 3*d*–4*f* coupling must be distinctly less developed than commonly assumed: It competes with other effects of comparable magnitude that can be associated to a different magnetic structure.

Consequently, a variety of phenomena that were related to a pronounced 3*d*–4*f* coupling have to be scrutinized. This includes the  $P\bar{6}_3cm \rightarrow P6_3cm$  reorientation of the Mn<sup>3+</sup> lattice in HoMnO<sub>3</sub> [5, 22], which plays a role in the emergence of a giant magnetoelectric effect [6]. Supplementary (or alternative) to Mn<sup>3+</sup>–Ho<sup>3+</sup> exchange the temperature dependence of the magnetic anisotropy or magnetoelastic effects [13] may be responsible for the reorientation. As another issue, R<sup>3+</sup> ordering in the high-temperature range cannot be due to straightforward induction by the Mn<sup>3+</sup> order since this would inevitably lead to compatible Mn<sup>3+</sup> and R<sup>3+</sup> order. Finally, we cannot confirm that the Mn<sup>3+</sup> order is directly determined by the size of the R<sup>3+</sup> ion and, thus, by the R<sup>3+</sup>–O<sup>2-</sup>–Mn<sup>3+</sup> bond angle [23]. If this were the case, the Mn<sup>3+</sup> spins in DyMnO<sub>3</sub> with the smallest R<sup>3+</sup> ion of the h-RMnO<sub>3</sub> system would order according to the  $P6_3cm$  structure already observed in HoMnO<sub>3</sub> and YMnO<sub>3</sub>. Likewise, it can be excluded that the unusual magnetic phase diagram and magnetoelectric properties established for HoMnO<sub>3</sub> [5, 22, 24] continue towards rare-earth h-RMnO<sub>3</sub> compounds with a smaller R<sup>3+</sup> radius than Ho<sup>3+</sup>. These observations, too, corroborate the relative independence of the Mn<sup>3+</sup> and R<sup>3+</sup> lattices.

In the low-temperature range and in a magnetic field applied along *z* the magnetic order of the Dy<sup>3+</sup> spins changes from  $P\bar{6}_3cm$  to  $P6_3cm$  [14, 17]. In the following the effect of this transition on the Mn<sup>3+</sup> spins is investigated. The emerging intensity of the (100) peak in Fig. 2 reflects the transition of the Dy<sup>3+</sup> lattice to the  $P6_3cm$  phase in agreement with Table I. However, it also obscures the Mn<sup>3+</sup>-related contributions so that we revert to SHG measurements for a unique identification of the Mn<sup>3+</sup> order.

Figure 1(d) and Fig. 3(c) show that the SHG intensity is quenched in the low-temperature range and in a magnetic field. According to Table I this indicates a transition to either the  $P6_3cm$  or the  $P\bar{6}_3cm$  phase. According to Figs. 3(a) and 3(b) the  $P\bar{6}_3cm \rightarrow P6_3cm$  transition passes through a state with  $P3\bar{c}$  symmetry for which  $\chi_{xxx} \neq 0$ ,  $\chi_{yyy} = 0$  while the  $P\bar{6}_3cm \rightarrow P6_3cm$  transition passes through a state with  $P3$  symmetry for which  $\chi_{xxx} \neq 0$ ,  $\chi_{yyy} \neq 0$  [18]. Figure 3(c) reveals

that the former scenario is realized. This is confirmed by the phase diagram in Fig. 3(d). Data points denote the magnetic field at which a magnetic phase transitions are observed with the gray area marking the difference between field-increasing and -decreasing runs. Qualitatively, the same phase diagram was obtained on h-RMnO<sub>3</sub> with  $R = \text{Er, Tm, Yb}$ , all of which exhibit a  $P\bar{6}_3cm \rightarrow P6_3cm$  transition of the Mn<sup>3+</sup> lattice in a magnetic field whereas the phase diagram of h-HoMnO<sub>3</sub>, in which this transition does not occur, is different. We conclude that in the low-temperature range and in a magnetic field along  $z$  the magnetic symmetry of the Mn<sup>3+</sup> lattice in h-DyMnO<sub>3</sub> is  $P6_3cm$  and, thus, compatible to the magnetic symmetry of the Dy<sup>3+</sup> lattice.

Nevertheless this compatibility is not a compulsory indication for an enhanced  $3d-4f$  exchange in the low-temperature range.  $P6_3cm$  is a ferromagnetic point group and the observation that a magnetic field supports the transition into this state indicates that the magnetic field energy rather than Mn<sup>3+</sup>-Dy<sup>3+</sup> exchange coupling may be responsible for the  $P\bar{6}_3cm \rightarrow P6_3cm$  transition of the Mn<sup>3+</sup> lattice. The field is generated internally by the ferromagnetic order of the Dy<sup>3+</sup> lattice and supported externally by the applied magnetic field. Accordingly, the gray area in Fig. 3(d) does not show the hysteresis of a first-order transition of the Mn<sup>3+</sup> lattice but rather the response of the Mn<sup>3+</sup> lattice to the magnetizing field exerted by the Dy<sup>3+</sup> lattice when it is ferromagnetically ordered.

We thus observed that the magnetic order of the manganese and the rare-earth sublattices in the h-RMnO<sub>3</sub> system can be incompatible from the point of view of symmetry. In h-DyMnO<sub>3</sub> Mn<sup>3+</sup> ordering according to the  $P\bar{6}_3cm$  symmetry and Dy<sup>3+</sup> ordering according to the  $P\bar{6}_3cm$  symmetry is revealed. The incompatibility demonstrates that the  $3d-4f$  interaction in the h-RMnO<sub>3</sub> series is distinctly less developed than assumed up to now. Even when the incompatibility is overcome by an internal or external magnetization field, pronounced Mn<sup>3+</sup>-Dy<sup>3+</sup> exchange does not have to be involved.

As a consequence, a variety of magnetoelectric coupling effects in the h-RMnO<sub>3</sub> system that were previously assigned to pronounced  $3d-4f$  coupling have now to be scrutinized with respect to their origin. Apparently, interactions *within* the Mn<sup>3+</sup> or R<sup>3+</sup> lattices as well as separate crystallography, anisotropy, and frustration effects play a greater role than expected up to now. In particular, externally induced polarization [6] or magnetization [22] fields rather than the Mn<sup>3+</sup>-R<sup>3+</sup> exchange may contribute substantially to the magnetoelectric response.

C.W., D.M., Th.L., and M.F. thank the DFG (SFB 608) for subsidy. D.N.A. thanks the DFG for financial support under Contract No. AR 613/1-1.

- 
- [\*] Email address: fiebig@hiskp.uni-bonn.de
- [2] M. Fiebig, *J. Phys. D* **38**, 123 (2005).
- [3] S.-W. Cheong and M. Mostovoy, *Nat. Mater.* **6**, 13 (2007).
- [4] R. Palai *et al.*, *Phys. Rev. B* **77**, 014110 (2008).
- [5] F. Yen *et al.*, *J. Mater. Res.* **22**, 2163 (2007).
- [6] Th. Lottermoser *et al.*, *Nature* **430**, 541 (2004).
- [7] X. Fabrèges *et al.*, *Phys. Rev. B* **78**, 214422 (2008).
- [8] S. Harikrishnan *et al.*, *J. Phys.: Condens. Matter* **21**, 096002 (2009).
- [9] Th. Lonkai, D. Hohlwein, J. Ihringer, and W. Prandl, *Appl. Phys. A*, **74**, S843 (2002).
- [10] H. Sugie, N. Iwata, and K. Kohn, *J. Phys. Soc. Jpn.* **71**, 1558 (2002).
- [11] I. Munawar and S. H. Curnoe, *J. Phys.: Condens. Matter* **18**, 9575 (2006).
- [12] S. Lee *et al.*, *Nature* **451**, 805 (2008).
- [13] X. Fabrèges *et al.*, *Phys. Rev. Lett.* **103**, 067204 (2009).
- [14] S. Nandi *et al.*, *Phys. Rev. B* **78**, 075118 (2008).
- [15] The four one-dimensional representations consistently explain our data so that two more two-dimensional representations denoting lower symmetries [7, 14, 22] are omitted.
- [16] S. Nandi *et al.*, *Phys. Rev. Lett.* **100**, 217201 (2008).
- [17] V. Yu. Ivanov *et al.*, *Phys. Solid State* **48**, 1726 (2006).
- [18] R. R. Birss, *Symmetry and Magnetism*, (North Holland, Amsterdam, 1966).
- [19] M. Fiebig, V. V. Pavlov, and R. V. Pisarev, *J. Opt. Soc. Am. B* **22**, 96 (2005).
- [20] B. Hillebrands, *J. Phys. D: Appl. Phys.* **41**, 160301 (2008).
- [21] T. Iizuka-Sakano, E. Hanamura, and Y. Tanabe, *J. Phys.: Condens. Matter* **13**, 3031 (2001).
- [22] M. Fiebig, Th. Lottermoser, and R. V. Pisarev, *J. Appl. Phys.* **93**, 8194 (2003).
- [23] D. P. Kozlenko *et al.*, *J. Phys.: Condens. Matter* **19**, 156228 (2007).
- [24] O. P. Vajk *et al.*, *Phys. Rev. Lett.* **94**, 087601 (2005).

TABLE I: Selection rules for SHG and neutron diffraction distinguishing between the four one-dimensional symmetry representations of the crystallographic space group  $P6_3cm$  of h-RMnO<sub>3</sub> [15].

Representation		$\Gamma_1, A_1$	$\Gamma_2, A_2$	$\Gamma_3, B_1$	$\Gamma_4, B_2$
Symmetry		$P6_3cm$	$P\bar{6}_3cm$	$P\bar{6}_3cm$	$P\bar{6}_3cm$
SHG	$\chi_{xxx}$	0	0	0	$\neq 0$
(Mn <sup>3+</sup> )	$\chi_{yyy}$	0	0	$\neq 0$	0
Neutron	(100)	58%	0	62%	0
(Mn <sup>3+</sup> )	(101)	17%	100%	17%	93%
Neutron	(100)	0	100%	0	75%
(Dy <sup>3+</sup> )	(101)	100%	0	2%	0

Symmetries refer to the magnetic structure of the Mn<sup>3+</sup> or Dy<sup>3+</sup> *sublattice*; the overall symmetry is determined by the intersection of the sublattice symmetries. Sketches of the magnetic structures of the Mn<sup>3+</sup> and Dy<sup>3+</sup> sublattices are given in Refs. 6 and 14. SHG selection rules were derived from Ref. 18. The neutron diffraction yield contributed by the Mn<sup>3+</sup> and the Dy<sup>3+</sup> order, respectively, was calculated as described in the text. The largest value obtained for each sublattice corresponds to 100%.



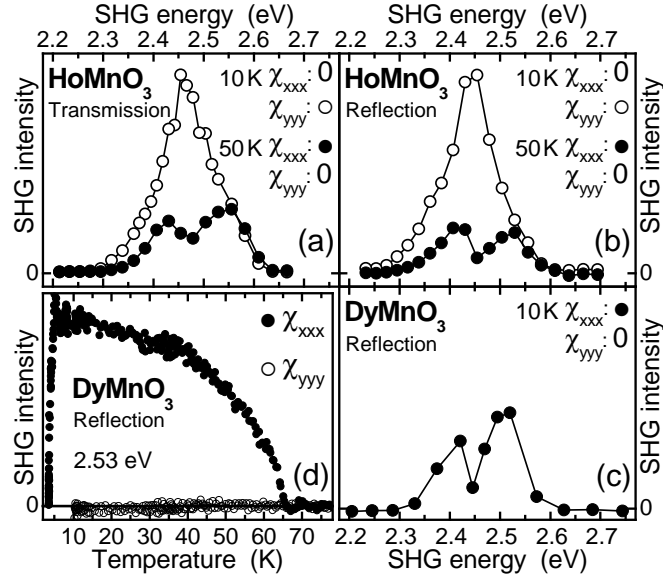


FIG. 1: Spectral, polarization, and temperature dependence of SHG in h-RMnO<sub>3</sub> compounds. A “0” indicates zero SHG intensity. (a, b) SHG spectra of h-HoMnO<sub>3</sub> measured in (a) transmission and (b) reflection with a fs laser. (c) SHG spectra of h-DyMnO<sub>3</sub> measured in reflection with a fs laser. (d) Temperature dependence of the signal in (c).

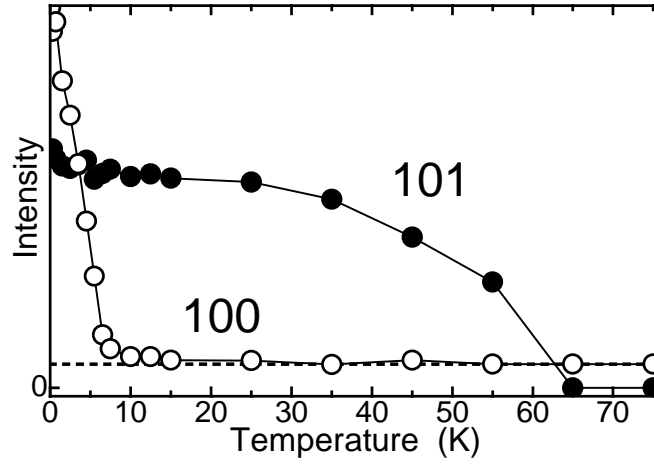


FIG. 2: Temperature dependence of the (101) and (100) reflections of h-DyMnO<sub>3</sub> measured in a cooling run on the sample from Fig. 1. The dashed line marks the offset due to crystallographic contributions.

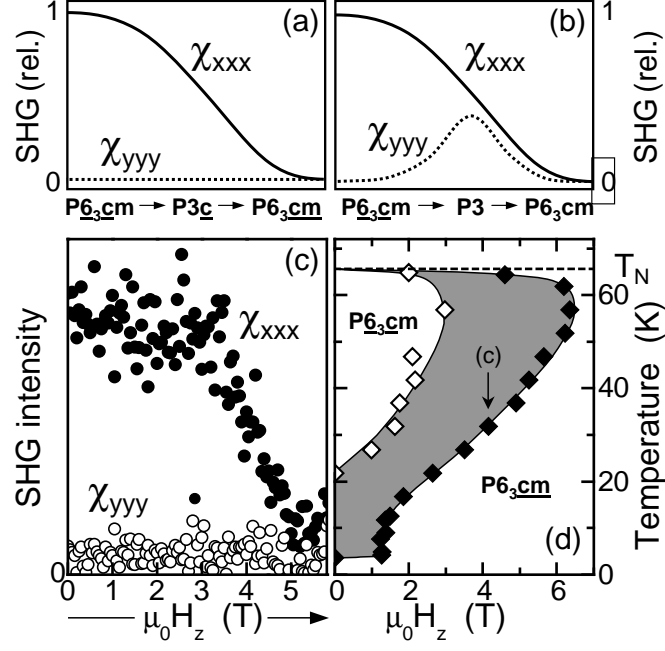


FIG. 3: Phase diagram of the magnetic  $Mn^{3+}$  order in h-DyMnO<sub>3</sub> exposed to a magnetic field along  $z$ . (a, b) Sketch of the SHG tensor contributions in the course of the spin reorientation towards the (a)  $P6_3cm$  and (b)  $P6_3cm$  phase. (c) Exemplary field dependence of the SHG signal at 32 K measured in a field-increasing run. (d) Phase diagram derived from measurements as in (c). Temperature-increasing and -decreasing runs yield the boundaries on the right- and left-hand side of the gray area, respectively. The boundary values correspond to observation of 50% of the SHG yield of the  $P6_3cm$  phase.